New insights into the aquatic photo-induced toxicity of nine sulfonamide antibiotics: Apparent photolysis, toxicity evolution and mechanisms

Linke Ge[a,b], Jiahui Wang[a], Andrew Sweetman[b], Zhixuan Zheng[a], Peng Zhang[a,*], Nannan Cui[a,*]

[a] *School of Environmental Science and Engineering, Shaanxi University of Science & Technology, Xi'an 710021, China*

[b] *Lancaster Environment Centre, Lancaster University, Lancaster LA1 4YQ, United Kingdom*

ABSTRACT

As newly recognized environmental contaminants, sulfonamide antibiotics (SAs) widely exist in aqueous systems and photo-degrade significantly in sunlit surface waters, requiring new insights into their aqueous apparent photolytic mechanisms and photo-modified toxicity. In this study, reaction kinetics, self-sensitized photo-oxidation, transformation pathways, antibacterial activity and photo-induced toxicity were investigated during the apparent photolysis of nine SAs including sulfamethoxazole (SMX), sulfisoxazole, sulfathiazole, sulfamethizole, sulfadimethoxine (SDM), sulfadiazine, sulfachloropyridazine, sulfamerazine and sulfamethazine. Under simulated sunlight irradiation (λ > 290 nm), most five-membered heterocyclic SAs underwent photodegradation at a faster rate than all six-membered heterocyclic SAs, which was ascribed to their chemical structures including different heterocyclic groups and associated substituents ($-CH_3$). The scavenging experiments indicated that SMX underwent self-sensitized photo-degradation via $O_2^{\bullet-}$, $^1O_2$ and •OH, and direct

* Corresponding author

E-mail addresses: zhangpeng4477@sust.edu.cn (P. Zhang), cuinannan@sust.edu.cn (N. Cui)

photo-degradation via $^3P^*$. The contribution of $O_2^{\bullet-}$ (40.71%−59.01%) and $^1O_2$ (29.13%) mediated self-sensitized photo-oxidation was found to be the highest under acidic and alkaline conditions, respectively. Photo-product identification was carried out with HPLC-MS^2, which identified proposed transformation pathways of five-membered heterocyclic SMX which involved photo-cleavage and photo-polymerization, while six-membered heterocyclic SDM underwent S−N bond cleavage, hydroxylation, desulfonation, methylation and addition reaction at sulfonyl-N. Based on multiple bioassays (*Escherichia coli* and *Vibrio fischeri*), the antibacterial activity changes and photo-modified toxicity evolution appeared to depend on dominant photo-degradation pathways and primary intermediates. Furthermore, the ECOSAR model confirmed the comparable or higher toxicities of the intermediates compared to the parent compounds. These findings provide new photochemical mechanistic insights into the large class of SAs, which allows a better assessment of their photochemical persistence, fate and risks in aquatic environments.

Keywords: sulfonamide antibiotics; self-sensitized photolysis; transformation products; antibacterial activity; photo-modified toxicity

1. Introduction

Antibiotics have been considered as a critical environmental issue due to their widespread occurrence, and potential harmful effects on microbial populations (Wang et al., 2024; Li et al., 2023). When discharged into wastewater streams, most antibiotics are incompletely removed by traditional treatment methods (Cao et al., 2024; Guo et al., 2025a), and as , they continuously enter aquatic environments they can be considered to show pseudo-persistence (Wei et al., 2024). Their persistence in aqueous systems may result in the propagation of antibiotic resistant bacteria with multiple drug resistance, posing a serious risk to aquatic systems and human health (Liu et al., 2023a; Hou et al., 2023). As a large important category of antibiotics,

sulfonamides (SAs) are extensively used in the aquaculture, animal husbandry and human health. They have been detected in aquatic environments through a variety of monitoring studies all over the world (Cao et al., 2024; Jia et al., 2023; Wang et al., 2023) (Table S1). Average concentrations in surface waters of rivers and adjacent seas of China have been reported to range from 0.1 to 150.83 ng L^{-1} (Fig. S1). Therefore, given the ubiquity of the antibiotic pollutants in aquatic systems, it is essential to explore their transformation in aqueous environments, as well as to evaluate the subsequent toxicity and risks to aquatic organisms.

Previous studies have investigated the ecotoxicological effects of SAs on aquatic biota (Li et al., 2025a; Huo et al., 2023; Zhu et al., 2021). By selectively inhibiting microorganisms in ecological systems, SA residues can demonstrably influence natural microbial communities (Välitalo et al., 2017), and result in ecotoxicological effects and resistance genes in microorganisms (Zainab et al., 2020). Interestingly, the photo-transformation of SAs was determined to have a important impact on their biological effects (Guo et al., 2021; Cheng et al., 2021; Ge et al., 2019). In sunlight-irradiated surface waters, apparent photo-chemical degradation is the main transformation pathway in determining the fate and risk of SAs (Tang et al., 2024),. Furthermore, photo-degradation irreversibly changes molecular structures, and results in the formation of transformation products (TPs) including reactive species and organic intermediates (Löffler et al., 2023; Kairigo et al., 2020). TPs may exhibit significantly different physiochemical properties and higher toxicity to organisms, urging the consideration of the photo-reaction types and photo-induced toxicity when assessing their environmental fate and ecological risks.

When irradiated by sunlight, aqueous organic pollutants can not only undergo direct photo-degradation via singlet and triplet excited states, but also undergo reactive-oxygen-species (ROS, e.g., •OH, $^1O_2$ and $O_2^{\bullet-}$) mediated self-sensitized photo-oxidation (Hsu et al., 2019; Zhang et al., 2018). These two distinct reactions collectively constitute an apparent photolysis

process. Clarifying the photo-reaction types and mechanisms is of great importance to assess their environmental persistence and understand the risks they may pose. Previous studies have reported apparent photo-degradation of SAs, showing that the photolytic efficiency of SAs was significantly affected by the solution pH (Oliveira et al., 2019; Vibha et al., 2025). However, it is not clear whether SAs undergo self-sensitized photo-oxidation, and which ROS might be involved in the reaction. Therefore, it is necessary to quantify the contribution of self-sensitized photo-degradation via ROS on their apparent photolysis at a range of pHs, and to reveal the reactivity of different dissociated SA forms towards these ROS.

As for photo-induced bioeffects of SAs, previous studies have reported photo-sensitized and photo-modified toxicities (Andino-Enríquez et al., 2025; Liu et al., 2023b; Zeng et al., 2021). When compared with the dark controls, the continuous exposure with simulated sunlight enhanced the acute toxicity of aqueous SAs to *Daphnia magna* (*D. magna*), attributing to the generation of ROS and the subsequent photo-sensitized toxicity of the parent compounds (Jung et al., 2008). As for the photo-modified toxicity of SAs, Xu et al. (2014) and Trovó et al. (2009) observed that the photo-degradation intermediates of SAs exhibited higher toxicity to *Vibrio fischeri* and greater antibacterial capacity to *D. magna* than the parent compounds, respectively. Similarly, Voigt et al. investigated the antimicrobial efficacy of photo-degraded SAs by determining their minimal inhibitory concentrations (MIC) to *Pseudomonas fluorescens* and *Bacillus subtilis* during the photo-degradation process, revealing that the MIC values of photolyzed SAs exhibited 2.5- to 5-fold increase compared to those of the parent compounds (Voigt et al., 2017). In addition, the inhibitory or stimulatory effects of photolytic products several SAs (sulfamethoxazole (SMX), sulfacetamide (SA), sulfadiazine (SD) and sulfathiazole (ST)) on the growth of *Calluna vulgaris* were also discovered (Zessel et al., 2014). These previous studies have demonstrated the photo-generated toxicity of SAs to non-target organisms, and provide theoretical support for new insights into the photo-induced toxicity of

SAs, though toxicity evolution and related mechanisms were not fully considered. To better assess the photo-degradation induced ecological risks of SAs, photochemical transformation products and pathways need to be identified, and the mechanisms of photo-induced toxicity should be clarified.

This study seeks new insights into self-sensitized photo-degradation, photo-degradation pathways, toxicity changes and mechanisms of nine SAs. These representative SAs selected as model compounds have been frequently detected in surface waters and known to undergo solar photo-degradation (Fig. S1) (Cao et al., 2024; Mac Loughlin et al., 2024). In order illustrate the photo-induced toxicity mechanisms of SAs, their aqueous photo-degradation kinetics and key by-products were investigated, along with an evaluation of their toxicity and antibacterial activity changes during the photo-transformation processes. The present study provides a comprehensive understanding of photochemical behavior and photo-modified toxicity of SAs, which are important to better assess the environmental fate and ecological risks of the emerging contaminants.

2. Materials and methods

2.1 Reagents and materials

Nine SAs (purity > 98 %) including SMX, sulfisoxazole (SIX), ST, sulfamethizole (SMT), SDM, SD, sulfachloropyridazine (SCP), sulfamerazine (SM) and sulfamethazine (SMZ) were obtained from different suppliers. The information related to SAs is given in Table S2. Isopropanol (IPA), acetonitrile (ACN) and methanol (MeOH) were of HPLC grade and purchased from Alfa Aesar and TEDIA (Fairfield, USA). Furfuryl alcohol (FFA, purity 98%) and benzoic acid (BA, 98%) were procured from J&K Technology Co., Ltd. Hydrogen peroxide (H_2O_2, 30%) was provided by Acros Organics. Other reagents such as benzoquinone were of analytically pure (at least 97% purity) and used as received. Beef extract, peptone and agar

powder were purchased from Beijing Aoboxing Biology Technology Co., Ltd. *Escherichia coli* (*E. coli*) and Freeze-dried *Vibrio fischeri* were supplied by the Shanghai Bioresource Collection Center and the Zhejiang Yangtze Delta Region Institute of Tsinghua Univ., respectively. To prepare photolytic solutions, ultrapure water (18.2 MΩ cm) was obtained with a Millipore Milli-Q® water purifier.

2.2 Photolytic experiments

The emission spectra of the light sources (Fig S2) and the absorption spectra of the model compounds (Fig S3) were determined by the Acton SP-300 monochromator (Princeton Instruments, Inc.) and TU1901 UV-Visible spectrophotometer (Beijing Purkinje General Instrument Co., Ltd.), respectively. To carry out the photochemical experiments, all solutions of individual SAs (C_0 = 10 μM) were pipetted into quartz tubes (vol. 50 mL, dia. 20 mm), and placed in photochemical reactor (Fig S4), of which the temperature was maintained at 25 °C. The solutions were irradiated with a high-pressure mercury lamp (500 W, λ > 290 nm), which was cooled and filtered by a Pyrex-well (Ge et al., 2023; Luo et al., 2019). Using a UV radiometer (Beijing Normal University photoelectric instrumental factory), the light intensities in the center of the solutions were measured to be 7.52 Mw cm^{-2} at 420 nm and 5.32 Mw cm^{-2} at 365 nm, respectively.

To determine if the SAs underwent self-sensitized photo-oxidation via •OH, $^1O_2$ and $O_2^{\bullet-}$ as well as direct photolysis via $^3P^*$, SMX was selected as a representative compound, and included RS scavenging experiments with IPA, triethylene diamine (DABCO), *p*-benzoquinone (*p*-BQ) and 2,4,6-trimethylphenol (TMP) were undertaken. With reference to a previous study (Cui et al., 2025), the oxidation reactivity of SA towards these RS was investigated using competing kinetic experiments. The methods for calculating the self-sensitized photo-oxidation contribution ratios (R_{ROS}) and bimolecular reaction rate constants are described in S1 and S2, respectively. These photolytic experiments and dark controls were carried out at least in

triplicate. In order to analyze the SA concentrations and identify the key transformation products, an Agilent 1260 HPLC and an Agilent 1260-6470B HPLC-MS/MS were employed, respectively. The analysis methods were detailed in the Text S3.

2.3 Antibacterial bioassay

The antibacterial activities of the SA photo-degradation solutions against *E. coli* were determined to clarify the changes of antibacterial activity as a result of their photo-degradation. The bioassay was performed in accordance with China standard method QB/T 2738-2012 (Ge et al., 2015), with *E. coli* as the indicator of vitro bacteriostatic experiment. The diameters of inhibition zone were determined as the index for antibacterial activity (Tao et al., 2010; Klančnik et al., 2010). The significant differences in antibacterial activity between the photolyzed and raw solutions of SAs were evaluated using one-way analysis of variance (ANOVA).

2.4 Biotoxicity experiment

The *Vibrio fischeri* bioassay was performed to assess the photo-induced toxicity evolution of SAs during the photo-degradation process. 15 min acute ecological toxicity was determined using an international standard method (ISO11348-3-2007), with test conditions optimized. Luminous intensities were measured using HACH Eclox water-quality detector (USA). The luminescence inhibition rates ($I\%$) were derived according to Eq. (1):

$$I\% = \frac{(I_0 - I_{15})}{I_0} \times 100\% \quad (1)$$

where I_0 and I_{15} stand for the luminescence intensities of the photo-degradation samples at 0 min and 15 min, respectively. Statistical significance was accessed at a level of $p = 0.05$ with SPSS version 27.0. In order to predict the photoinduced risk to multi-level organisms, the acute toxicity of individual SAs and photolytic products to fish, daphnia, and algae was evaluated using the Ecological Structure Activity Relationship model (ECOSAR, version 2.2).

3. Results and discussion

3.1 Apparent photolysis kinetics

No significant loss of SAs was found in dark controls, suggesting that the antibiotic compounds selected for study were unaffected by other degradation reactions (e.g., thermal or hydrolytic degradation) during the photolytic experiments. However, the nine SAs absorbed the actinic portion of illumination lights and suffered from rapid photo-degradation under simulated sunlight (λ > 290 nm). The parent SA concentrations were confirmed to underfo logarithmic decay during the attenuation by photo-degradation, indicating that the reaction followed pseudo-first-order kinetics with a good linear regression ($r^2 > 0.95$) between $\ln(C/C_0)$ and time (t). Their kinetic rate constants (k) and half-lives ($t_{1/2}$) are provided in Table S3. The corresponding logarithmic decay of the nine SAs has been plotted in Fig. 1. When comparing their photo-degradation kinetics of the study chemicals, SMX photo-degradation was the fastest ($k = (35.4 \pm 3.1) \times 10^{-3}$ min^{-1}) among SAs with five-membered heterocycle groups, followed by SIX, ST and SMT. Whereas, among SAs with six-membered heterocyclic groups, SDM photo-degradation was the fastest ($k = (13.8 \pm 0.7) \times 10^{-3}$ min^{-1}), followed by SD, SCP, SM and SMZ. The $t_{1/2}$ values of nine SAs increased by one order of magnitude from 12.2 min for SMX to 153.3 min for SMT.

The observations in Fig. 1 demonstrated the apparent photolytic difference across the nine SAs, which can be distinguished based on their chemical structures (Table S2). SAs contain an identical backbone structure (sulfanilamido group) but differ solely in their heterocyclic substituents. Thus, these heterocyclic groups and associated substituents are key determinants of the distinct photochemical behavior of various SAs in water. Generally, the photolytic rates of most SAs (i.e. ST, SIX, SMX) with five-membered heterocycle groups were faster than all SAs (i.e., SMZ, SM, SCP, SD, SDM) with six-membered heterocycle groups. Furthermore, the SA degradation kinetics were found to be also dependent on the number of methyl groups

197 ($-CH_3$) associated in the similar heterocyclic groups. For instance, the SAs with similar
198 heterocycle groups (five-membered heterocyclic SMX and SIX; six-membered heterocyclic SD,
199 SM and SMZ), the rate constant *k* decreased relative to the increase of the $-CH_3$ numbers. In
200 previous studies, faster photo-degradation rates for the five-membered heterocyclic SAs were
201 also observed across several SAs (Voigt et al., 2017; Boreen et al., 2005; 2004). However, the
202 influence of associated $-CH_3$ numbers on the photolysis rateswas under-represented in the
203 literature. The kinetic dependence on chemical structure suggested that SAs might photo-
204 degrade at rates based on heterocyclic groups and associated substituents (Boreen et al., 2004;
205 Zhou et al., 2019). Whereas, the proposed photolytic site needs to be verified by the product
206 identification of SAs.

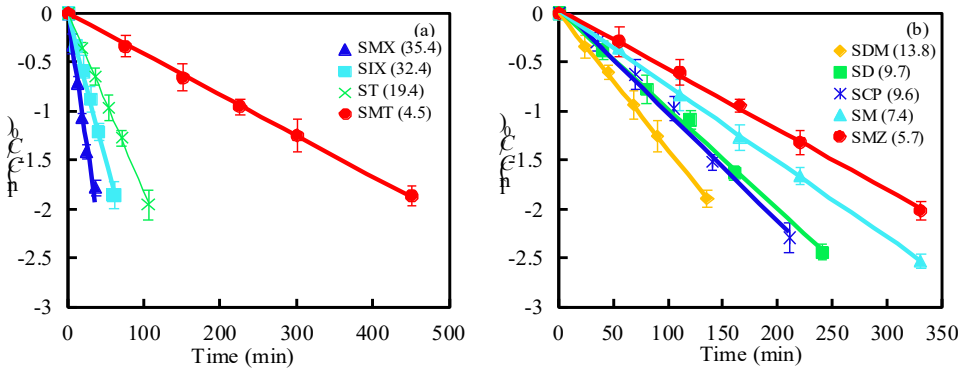

207

208 **Fig. 1.** Apparent photo-degradation kinetics of nine SAs (rate constants $k \times 10^3$ min^{-1}) under simulated
209 sunlight irradiation: (a) SAs with five-membered heterocycle groups; (b) SAs with six-membered
210 heterocyclic groups.

211 *3.2 Contribution of self-sensitized photo-oxidation*

212 As shown in Fig. S5, it is hypothesized that SAs undergo direct photo-degradation via excited
213 singlet ($^1SAs^*$) and triplet states ($^3P^*$), as well as self-sensitized photo-degradation initiated by
214 reactive oxygen species (ROS, e.g., •OH, $^1O_2$ and $O_2^{\bullet-}$) during their apparent photolysis. Herein,
215 these ROS are generated through energy transfer from $^3P^*$ to H_2O or dissolved O_2. To verify the
216 hypothesis, the ROS and $^3P^*$ scavenging experiments were carried out using SMX as a
217 representative SA. As shown in Fig. 2, the addition of IPA (•OH scavenger), DABCO (•OH/$^1O_2$

scavenger), *p*-BQ ($O_2^{\bullet-}$ scavenger) and TMP ($^3P^*$ scavenger) induced pronounced inhibitions of SMX photo-degradation of (p <0.05). It was demonstrated that SMX not only suffered from the self-sensitized photo-oxidation via •OH, $^1O_2$ and $O_2^{\bullet-}$, but also underwent direct photo-degradation via $^3P^*$. The scavenging reaction kinetic parameters (k and $t_{1/2}$), as shown in Table S4, were found to be dependent on solution pH (2, 5 and 8).

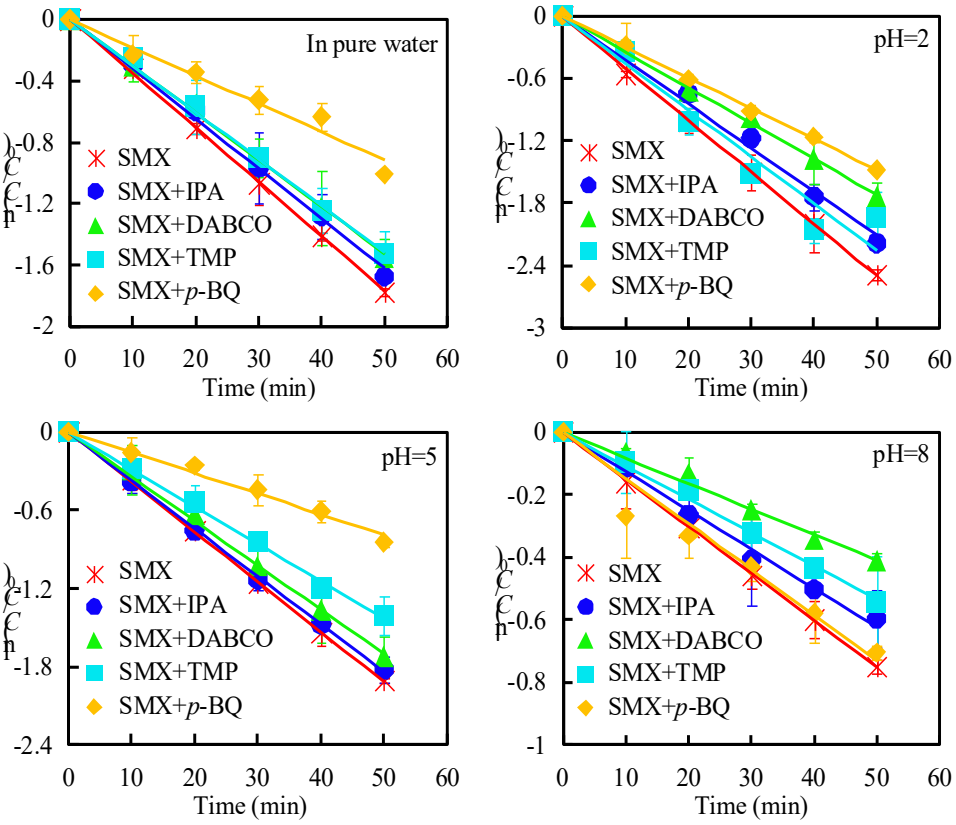

Fig. 2. The effects of adding different scavengers on apparent photolysis of SMX in pure water and at different pHs.

Furthermore, the data demonstrated that the contribution from different micro-reactions ($R_{\bullet OH}$, $R_{^1O2}$, $R_{O2^{\bullet-}}$ and $R_{^3P^*}$) to SMX apparentphotolysis under different conditions were quantified (Table 1). The contribution of $O_2^{\bullet-}$ induced self-sensitized photo-oxidation (40.71%−59.01%) was verified to be higher than that of all other reactive species in pure water and under acidic conditions (pHs 2 and 5), implying that $O_2^{\bullet-}$ played a major role in the self-sensitized photo-degradation of SMX. This can be attributed to the acidic solutions facilitating the generation of $O_2^{\bullet-}$ from $^3P^*$, and subsequently enhancing oxidation of SMX towards $O_2^{\bullet-}$. However, the

contribution of $^1O_2$ mediated self-sensitized photo-oxidation (29.13%) was the highest at pH 8. This suggested the increasing formation of $^1O_2$ from $^3P^*$ in the alkaline conditions. This phenomenon can be ascribed to the pH effect on the dissociated forms of the model compound SMX, which in turn altered the contribution of ROS mediated self-sensitized photo-oxidation (Ge et al., 2025a).

Table 1

The contribution rates (R_{RS}) of self-sensitized photo-degradation via ROS and direct photo-degradation via $^3P^*$ to apparent photolysis of SMX in pure water and under different pH conditions.

Reaction conditions	$R_{\bullet OH}$	$R_{^1O2}$	$R_{O2\bullet-}$	$R_{^3P*}$
Pure water	8.19%	5.64%	48.30%	14.41%
pH = 2	15.56%	15.76%	40.71%	9.78%
pH = 5	3.65%	7.31%	59.01%	25.32%
pH = 8	17.21%	29.13%	3.31%	28.47%

Although •OH was not the dominant ROS for SMX degradation under the range of pH values (Table 1), it was still anticipated to efficiently react with SMX in sunlit surface waters due to its high reactivity and non-selectivity (Kolasinski, 2025). At various pHs, the bimolecular reaction rates constants ($k_{RS,SMX}$) were determined to quantify the reactivity of SMX towards •OH, $^1O_2$ and $^3P^*$ (Tables S5 and S6). It was observed that the $k_{RS,SMX}$ values exhibited a significant pH dependence (p <0.05), with the highest oxidation reactivity of SMX towards •OH, $^1O_2$ and $^3P^*$ at pH 8. This was attributed to the different molecular morphologies and deprotonation degrees at various pHs (Ge et al., 2019; Ge et al., 2024). These apparent photolytic reactions might act on the photochemical risk and fate of SAs, urging further research into their transformation pathways and photo-modified toxicity.

3.3 Photo-transformation products and pathways

Based on the chromatographic separation and mass spectrometry analysis, the evolution of

thirty-three intermediates with time shown is in Fig. 3. The chromatographic peak areas of ST-P3, SMT-P3 and SMT-P4 showed a parabolic tendence , characterized by an initial rise and a subsequent decline in their abundance. The peak areas of SD-P2, SD-P5, SM-P2 and SM-P3 showed no significant increase with extended illumination time. These trends indicated that these intermediates were photo-reactive and underwent further photo-degradation. As for SMX-P1, SDM-P1, SCP-P2 and SM-P1, their peak abundance increased with irradiation time, suggesting lower reactivity of these products towards light exposure. Furthermore, given the higher degradation rates (apparent photolytic kinetics shown in Fig. 1), SMX and SDM were selected as model compounds to investigate their photo-degradation intermediates and transformation pathways under simulated solar irradiation. Their total ion currents (TIC) are shown in Fig. S6, from which eight significant intermediates were identified from SMX and SDM. The molecular weights (*Mw*), retention times (t_R) and MS fragment *m/z* are summarized in Table S7 and Fig. S7. As illustrated in Fig. 4, their corresponding chemical structures and photo-transformation pathways are proposed.

The photo-transformation of SMX with five-membered heterocyclic groups mainly involved two pathways: photo-cleavage and photo-polymerization (Fig. 4). In the photo-cleavage pathway (Path 1), apparent photolysis occurs via S−N bond cleavage, yielding sulfanilic acid (SMX-P2) as a common byproduct (Boreen et al., 2004). In Path 2, SMX-P3 was formed through addition reaction at the sulfonyl-N site. As for SDM containing six-membered heterocyclic substituents, four photo-degradation pathways were identified. In Path 1, the transformation pathways mainly involved cleavage of S−N bond (SDM-P1), hydroxylation and desulfonation (SDM-P4). Hydroxylation is due to the presence of the electron-rich aniline moiety, which in turn enables further •OH addition (Shah and Hao, 2017; Bilea et al., 2024). In Path 2, SDM was primarily transformed into a desulfonation product (SDM-P2) with the loss of SO_2. The mechanism for SO_2 extrusion involved the aromatic nucleophilic substitution of an

aniline radical cation, followed by a Smiles rearrangement (Ji et al., 2017). Furthermore, this pathway also involved the amino-N removal. In Path 3, SDM first suffered methylation, and then underwent addition reaction at sulfonyl-N, yielding SDM-P3. In Path 4, SDM was primarily transformed into SDM-P5 via the introduction of a $-OCH_3$ to the six-membered heterocyclic group. Combined with the abundant detection of photo-products (Fig. 3), the photo-cleavage process with cleavage of S−N bond was confirmed as the primary transformation pathway for SMX and SDM.

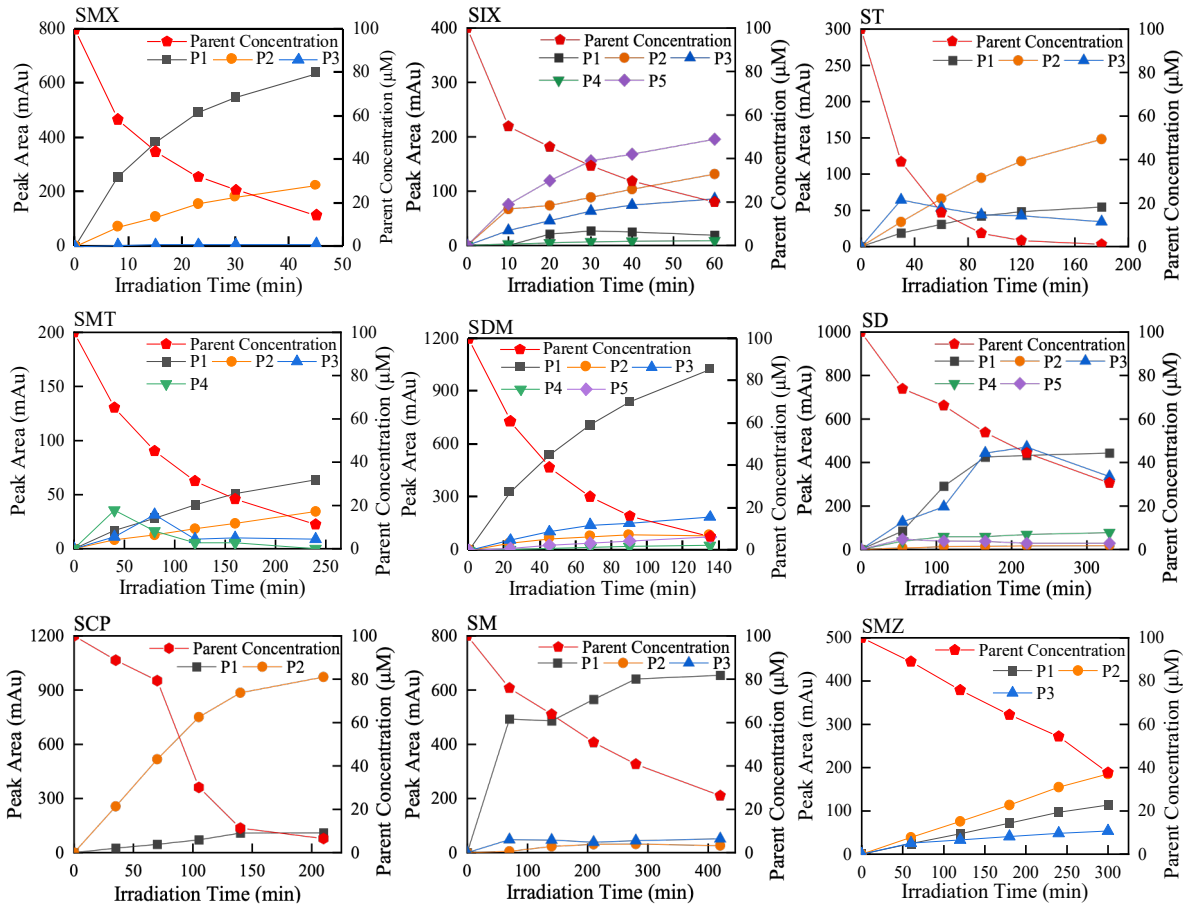

Fig. 3. The abundance and evolvement of main photo-products (peak area) and during the photo-degradation of nine SAs (parent concentration)

In environmental surface waters, SAs have been shown to be ubiquitous and would undergo many photochemical reactions including the apparent photolysis (Hernández-Tenorio, 2024; Loureiro Dos Louros et al., 2020) and ROS-induced sensitized photo-degradation (Andino-Enríquez et al., 2025; Liu et al., 2023b; Qin et al., 2024). However, results from this present

study elucidated the multifarious photolytic intermediates and pathways of SAs, providing fundamental insights into the phototransformation fate of this class of organic contaminants. It is worth noting that the photochemical reactions did not initially affect the main backbone structure of the SAs, suggesting that their antibacterial capacity might persist in those intermediates (Niu et al., 2017).Therefore, it is necessary to further examine the antimicrobial activities and biology toxicity of these transformation products.

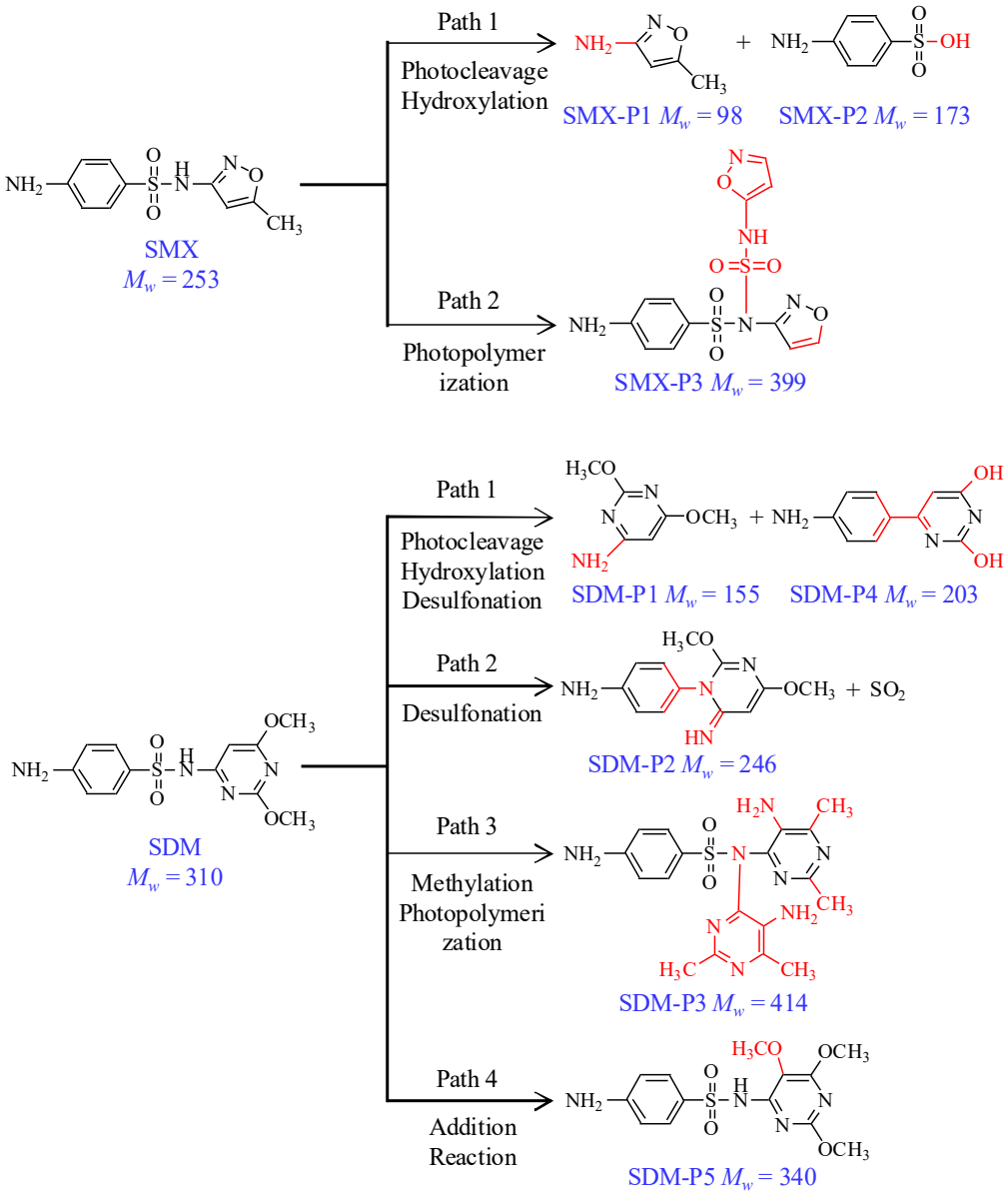

Fig. 4. Transformation products and pathways for apparent photo-degradation of five-membered heterocyclic SMX and six-membered heterocyclic SDM under simulated sunlight irradiation.

3.4 Changes in antibacterial activities against E. coli

306 The antibacterial activities of nine SAs were evaluated using *E. coli* as a bioindicator. As
307 depicted in Fig. S8, the initial antibacterial activities of raw SMX, SD and SM (10.31 mm,
308 10.20 mm and 11.50 mm respectively) were higher ($p < 0.05$) than those of the other 6 SAs
309 which range from 8.49 mm to 9.52 mm. This higher activity can be attributed to their lower
310 molecular weights, which reduces steric hindrance and facilitates their entry into *E. coli* cells,
311 thereby producing more significant antibacterial effects (Baek et al., 2019).
312 During apparent photolysis of SAs (Fig. 5), the antibacterial activities evolved in distinct
313 patterns as the parent compounds decayed and intermediates were formed. With increasing
314 illumination time, the antibacterial activities of ST and SD against *E. coli* showed a general
315 declining trend and lower than their initial values ($p < 0.05$). However, the antibacterial
316 activities of other SAs exhibited a fluctuating pattern. SDM and SCP first showed an increase
317 followed by a decrease in antibacterial activities ($p < 0.05$) at the initial illumination period.
318 This suggested that the two SAs generated photo-modified products with notable antibacterial
319 activities against *E. coli*. In comparison, the other five SAs displayed a significant decrease
320 followed by an increase ($p < 0.05$), indicating that short-time illumination reduced their
321 antibacterial activities. However, extending illumination time induced the formation of
322 antibacterial photo-products, which might be generated from photo-transformation pathways
323 (Fig. 4). Thus, the antibacterial activity evolution during the photo-degradation of SAs are
324 dependent on primary products and pathways. As for other classes of antibiotics, many photo-
325 transformation products of fluoroquinolone (FQs) and tetracycline (TCs) also exhibited
326 antibacterial activity against *E. coli*. (Huang et al., 2025; Guo et al., 2025b).
327 Apart from antibacterial activity, toxicity assessment is a critical component of the
328 environmental risk assessment for aquatic contaminants (Ge et al., 2025b; Ge et al., 2025c).
329 Therefore, it is essential to further evaluate the changes in toxicity of SAs to *Vibrio fischeri*, to
330 predict the toxicity of individual photo-products to multiple-level aquatic organisms.

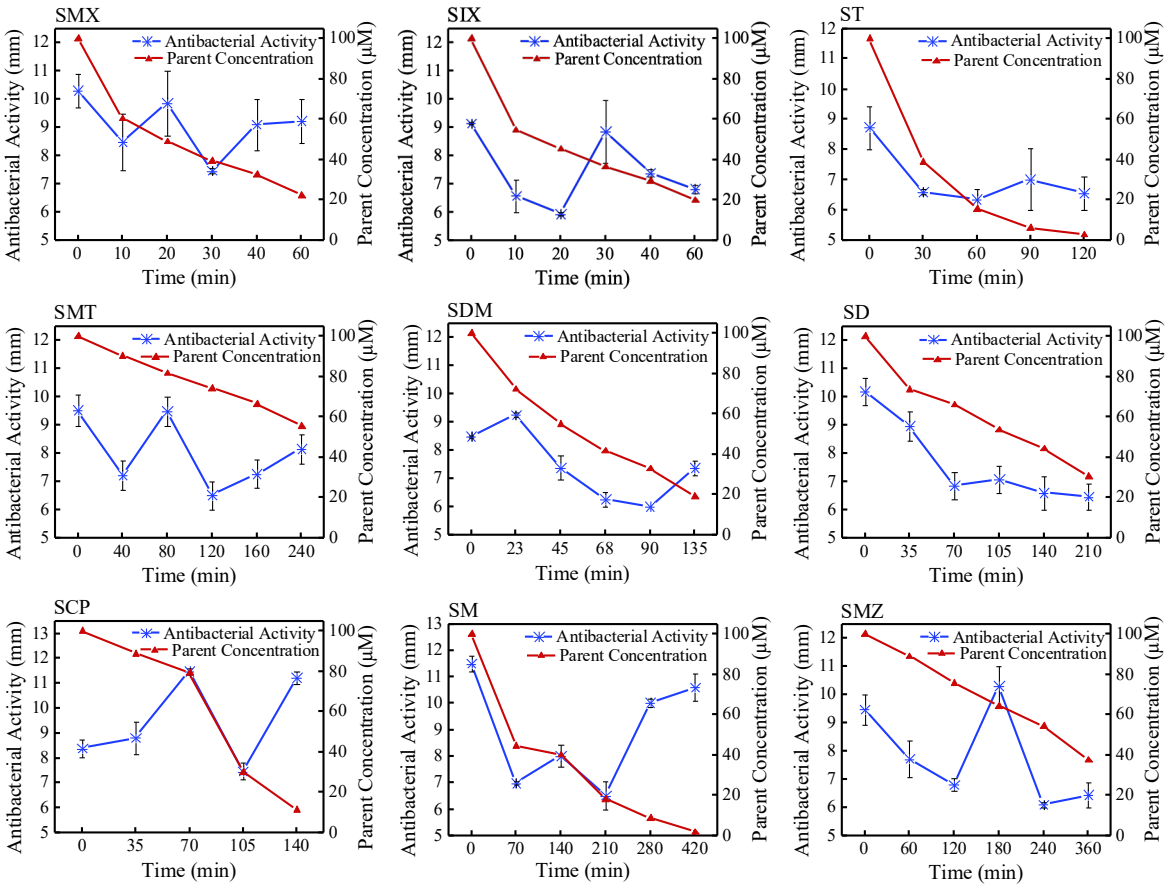

Fig. 5. Changes of nine SAs parent concentrations and antibacterial activity of the photo-degradation solutions to *E. coli* with irradiation time in water. The y-axis represents the agar plated bacteria-free zone diameter.

3.5 Photo-modified toxicities to Vibrio fischeri

The toxicities of the nine parent SAs were first assessed using *Vibrio fischeri*. As shown in Fig. 6, their luminescence inhibition rates (*I*%) ranged from 16.64% for SDM to 33.58% for SMT. During the apparent photo-degradation, their *I*% values exhibited diverse evolution curves with the declining concentrations of the parent compounds. The observed toxicity fluctuations were a result of the continuous formation and degradation of intermediates with varying toxicity. In most cases, the maximal *I*% values of the photolytic solutions were observably greater than those of the raw SAs ($p < 0.05$), indicating the formation of more toxic photo-products. Furthermore, the toxicity of individual products was assessed by ECOSAR version 2.2 software. Based on the results (acute toxicity and chronic toxicity) shown in Table

S8, it can be seen that SMX and SDM photo-transformed into several intermediates with comparable or higher toxicity, such as SMX-P1 and SDM-P4. Importantly, the toxicity results agreed well with the *Vibrio fischeri* bioassay.

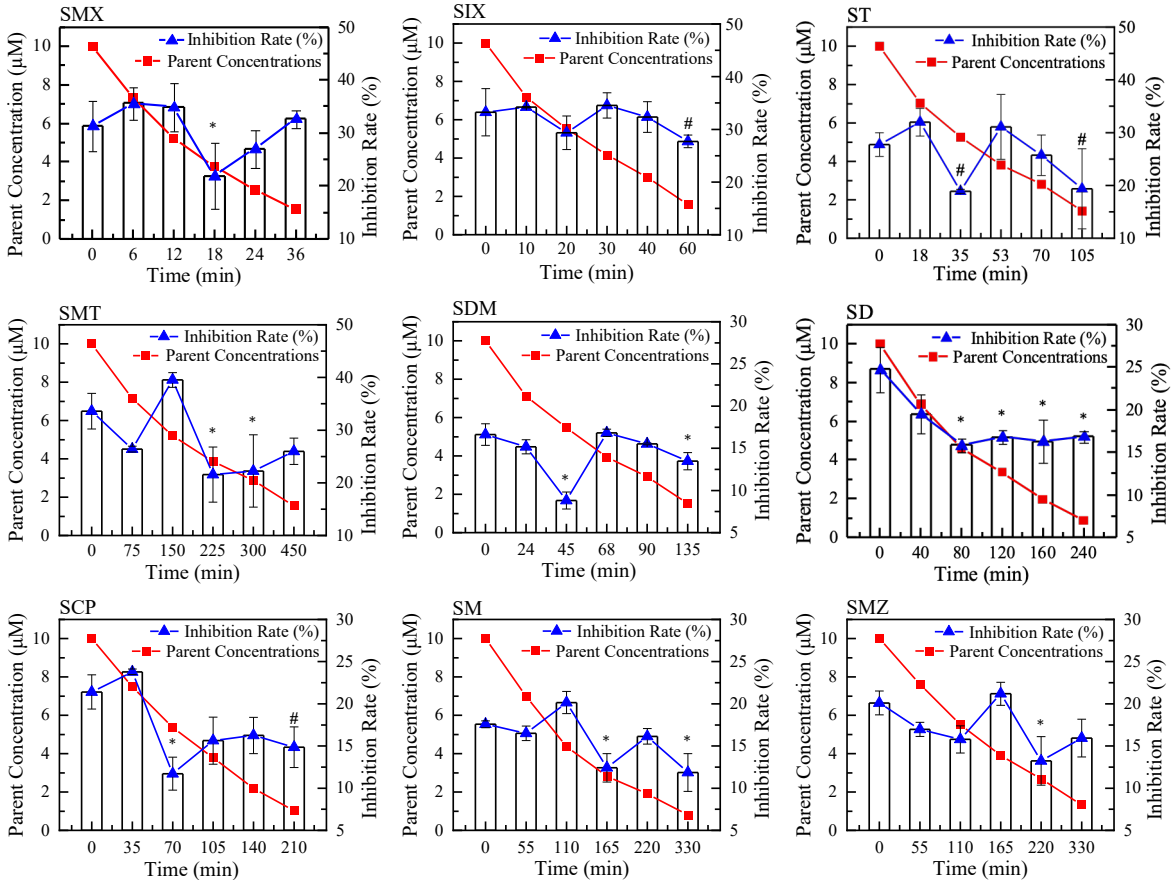

Fig. 6. Time-dependent changes in parent SA concentrations and luminescence inhibition rates to *Vibrio fischeri* during photolysis.

According to the photo-degradation products and primary pathways (Fig. 4), a mechanism for toxicity evolvement has been proposed. The cleavage of the sulfonamide bond (S−N) increases the number of $-NH_2$ groups that interact with *flavin mononucleotide*, a significant process for the luminescence inhibition of *Vibrio fischeri* (Jablonski and DeLuca, 1978). Meanwhile, the reduction in molecular weight and steric hindrance from photo-cleavage can facilitate penetration into *Vibrio fischeri* cells, thus promoting the observed increase in toxicity (Park et al., 2023). Moreover, products of addition reactions such as SDM-P4 are likely to exhibit higher toxicity than their parent compounds. Consequently, given the photo-enhanced

potential threat of the intermediates to aquatic systems, evaluating the photo-modified toxicity of emerging contaminants like SAs should be included in their environmental risk assessment (Ge et al., 2025a; Zheng et al., 2025).

4. Conclusion

This research provides a comprehensive investigation of the reaction kinetics, self-sensitized photo-oxidation, transformation pathways, antibacterial activity changes and photo-induced toxicity during the apparent photo-degradation process of nine widely detected SAs in the aqueous environment. Although their apparent photo-degradation followed pseudo-first-order kinetics ($t_{1/2}$ = 12.2−153.3 min), most SAs (i.e. ST, SIX, SMX) with five-membered heterocycle groups photodegraded faster than all SAs (i.e., SMZ, SM, SCP, SD, SDM) with six-membered heterocycle groups. This apparent photolytic difference can be ascribed to their different chemical structures including diverse heterocyclic groups and associated substituents (e.g., $-CH_3$). As a representative, SMX not only underwent self-sensitized photo-oxidation via $O_2^{\bullet-}$, $^1O_2$ and •OH, but also experienced direct photo-degradation via $^3P^*$. The contribution of $O_2^{\bullet-}$ (40.71%−59.01%) and $^1O_2$ (29.13%) mediated self-sensitized photo-oxidation was confirmed to be the highest under acidic and alkaline conditions, respectively, which was attributed to the different deprotonation degrees and RS reactivity at various pHs. Through the apparent photo-reactions, these SAs transformed into intermediates with different photo-reactivity. The transformation pathways of five-membered heterocyclic SMX involved photo-cleavage and photo-polymerization, while six-membered heterocyclic SDM underwent cleavage of the S−N bond, hydroxylation, desulfonation, methylation and addition reaction at sulfonyl-N. Furthermore, both the antibacterial activity changes and photo-modified toxicity evolution were found to be dependent on dominant photo-degradation pathways and primary intermediates. Importantly, the toxicity predictions from the ECOSAR software for the individual intermediates agreed with the *Vibrio fischeri* bioassay results.

This study not only filled a critical gap in understanding the RS-mediated apparent photolytic mechanisms of SAs in aqueous systems but also revealed their pathway-dependent antibacterial activity changes and toxicity evolution during the apparent photo-degradation. These findings are essential for accurately assessing the photochemical persistence, fate, and ecological risks of the emerging contaminants in aquatic systems. Furthermore, the clarified transformation mechanisms and photo-modified toxicity of SAs help to better understand the persistence and risks posed by SAs and key products in photo-assisted advanced oxidation processes (Felis et al., 2024; Duan et al., 2022; Li et al., 2025b).

CRediT authorship contribution statement

Linke Ge: Writing − review & editing, Conceptualization, Funding acquisition. **Jiahui Wang:** Writing − original draft, Data curation. Andrew Sweetman**:** Writing − review & editing. **Zhixuan Zheng:** Data curation. **Peng Zhang:** Writing − review & editing. **Nannan Cui:** Writing − review & editing.

Declaration of competing interest

The authors declare that they have no known competing financial interests or personal relationships that could have appeared to influence the work reported in this paper.

Acknowledgements

This work was supported by the Key Research and Development Program of Shaanxi Province (2024SF-YBXM-567), the National Natural Science Foundation of China (21976045, 22076112), Qingdao Key Laboratory of Analytical Technology Development and Offshore Eco-Environment Conservation (QDAE2503), Hainan Key Laboratory for Coastal Marine Eco-environment and Carbon Sink (2025SYSKFKT06), and the China Scholarship Council (CSC)

(202308610123).

Appendix A. Supplementary data

Supplementary data to this article can be found online at https://doi.org/*****/j.

References

Wang, C., Mao, Y., Zhang, L., et al. 2024. Insight into environmental adaptability of antibiotic resistome from surface water to deep sediments in anthropogenic lakes by metagenomics. Water Res. 256, 121583. https://doi.org/10.1016/j.watres.2024.121583

Li, J., Qiu, X., Ren, S., et al. 2023. High performance electroactive ultrafiltration membrane for antibiotic resistance removal from wastewater effluent. J. Membr. Sci. 672, 121429. https://doi.org/10.1016/j.memsci.2023.121429

Cao, S., Zhang, P., Halsall, C., et al. 2024. Occurrence and seasonal variations of antibiotic micro-pollutants in the Wei River, China. Environ. Res. 252, 118863. https://doi.org/10.1016/j.envres.2024.118863

Guo, X.M., Lu, X.M., Jia, J.W., et al. 2025a. Comprehensive assessment of 45 antibiotics in ten urban wastewater treatment plants in Northeastern China: Terminal treatment is not a reliable guard. J. Hazard. Mater. 489, 137755. https://10.1016/j.jhazmat.2025.137755

Wei, L., Su, Z., Yue, Q., et al. 2024. Microplastics, heavy metals, antibiotics, and antibiotic resistance genes in recirculating aquaculture systems. TRAC-Trend Anal. Chem. 172, 117564. https://doi.org/10.1016/j.trac.2024.117564

Liu, H., Shan, X., Song, L., et al. 2023a. An integrated multimedia fate modeling framework for identifying mitigation strategy of antibiotic ecological risks: A case study in a peri-urban river. Environ. Res. 238, 117225. https://doi.org/10.1016/j.envres.2023.117225

Hou, J., Long, X., Wang, X., et al. 2023. Global trend of antimicrobial resistance in common bacterial pathogens in response to antibiotic consumption. J. Hazard. Mater. 442, 130042. https://doi.org/10.1016/j.jhazmat.2022.130042

Jia, W.-L., Song, C., He, L.-Y., et al. 2023. Antibiotics in soil and water: Occurrence, fate, and risk. Curr. Opin. Environ. Sci. Health. 32, 100437. https://doi.org/10.1016/j.coesh.2022.100437

Wang, J., Lu, X., Jing, Q., et al. 2023. Spatiotemporal characterization of heavy metal and antibiotics in the Pearl River Basin and pollutants removal assessment using invasive

species-derived biochars. J. Hazard. Mater. 454, 131409. https://doi.org/10.1016/j.jhazmat.2023.131409

Li, S., Wang, R., Zhang, Y., et al. 2025a. Ecological risks of sulfonamides and quinolones degradation intermediates: Toxicity, microbial community, and antibiotic resistance genes. Bioresour. Technol. 418, 131967. https://doi.org/10.1016/j.biortech.2024.131967

Huo, W.-B., Jia, P.-P., Li, W.-G., et al. 2023. Sulfonamides (SAs) exposure causes neurobehavioral toxicity at environmentally relevant concentrations (ERCs) in early development of zebrafish. Aquat. Toxicol. 261, 106614. https://doi.org/10.1016/j.aquatox.2023.106614

Zhu, F., Pan, J., Zou, Q., et al. 2021. Electron beam irradiation of typical sulfonamide antibiotics in the aquatic environment: Kinetics, removal mechanisms, degradation products and toxicity assessment. Chemosphere 274, 129713. https://doi.org/10.1016/j.chemosphere.2021.129713

Välitalo, P., Kruglova, A., Mikola, A., et al. 2017. Toxicological impacts of antibiotics on aquatic micro-organisms: A mini-review. Int. J. Hyg. Environ. Health 220(3), 558-569. https://doi.org/10.1016/j.ijheh.2017.02.003

Zainab, S.M., Junaid, M., Xu, N., et al. 2020. Antibiotics and antibiotic resistant genes (ARGs) in groundwater: A global review on dissemination, sources, interactions, environmental and human health risks. Water Res. 187, 116455. https://doi.org/10.1016/j.watres.2020.116455

Guo, Z., Wang, J., Chen, X., et al. 2021. Photochemistry of dissolved organic matter extracted from coastal seawater: Excited triplet-states and contents of phenolic moieties. Water Res. 188, 116568. https://doi.org/10.1016/j.watres.2020.116568

Cheng, Z., Zuo, Z., Yang, S., et al. 2021. Study of free nitrous acid (FNA)-based elimination of sulfamethoxazole: Kinetics, transformation pathways, and toxicity assessment. Water Res. 189, 116629. https://doi.org/10.1016/j.watres.2020.116629

Ge, L., Zhang, P., Halsall, C., et al. 2019. The importance of reactive oxygen species on the aqueous phototransformation of sulfonamide antibiotics: Kinetics, pathways, and comparisons with direct photolysis. Water Res. 149, 243-250. https://doi.org/10.1016/j.watres.2018.11.009

Tang, G., Chen, Y., Lin, S., et al. 2024. The photo- and microbial degradation kinetics and pathways of sulfadoxine in seawater elucidated by liquid chromatography coupled with time-of-flight mass spectrometry. Chemosphere 351, 141225. https://doi.org/10.1016/j.chemosphere.2024.141225

Löffler, P., Escher, B.I., Baduel, C., et al. 2023. Antimicrobial transformation products in the qquatic environment: Global occurrence, ecotoxicological risks, and potential of antibiotic resistance. Environ. Sci. Technol. 57(26), 9474-9494. https://doi.org/10.1021/acs.est.2c09854

Kairigo, P., Ngumba, E., Sundberg, L.-R., et al. 2020. Occurrence of antibiotics and risk of antibiotic resistance evolution in selected Kenyan wastewaters, surface waters and sediments. Sci. Total Environ. 720, 137580. https://doi.org/10.1016/j.scitotenv.2020.137580

Hsu, M.H., Tsai, C.J. and Lin, A.Y. 2019. Mechanism and pathways underlying the self-sensitized photodegradation of methotrexate under simulated solar irradiation. J. Hazard. Mater. 373, 468-475. https://doi.org/10.1016/j.jhazmat.2019.03.095

Zhang, Y.N., Zhou, Y., Qu, J., et al. 2018. Unveiling the important roles of coexisting contaminants on photochemical transformations of pharmaceuticals: Fibrate drugs as a case study. J. Hazard. Mater. 358, 216-221. https://doi.org/10.1016/j.jhazmat.2018.06.068

Oliveira, C., Lima, D.L.D., Silva, C.P., et al. 2019. Photodegradation of sulfamethoxazole in environmental samples: The role of pH, organic matter and salinity. Sci. Total Environ. 648, 1403-1410. https://doi.org/10.1016/j.scitotenv.2018.08.235

Vibha, K., Prachalith, N.C., Kumar, H.M.S., et al. 2025. Utilizing sulfa drugs' pH-dependent spectral modifications for designing molecular logic gates. Spectrochim. Acta. A. Mol. Biomol. Spectrosc. 325, 125099. https://doi.org/10.1016/j.saa.2024.125099

Andino-Enríquez, M.A., Fabbri, D., Vione, D., et al. 2025. Photoinduced transformation pathways of the sulfonamide antibiotic sulfamethoxazole, relevant to sunlit surface waters. Environ. Pollut. 384, 126947. https://doi.org/10.1016/j.envpol.2025.126947

Liu, J., Xue, S., Jiang, C., et al. 2023b. Effect of dissolved organic matter on sulfachloropyridazine photolysis in liquid water and ice. Water Res. 246, 120714. https://doi.org/10.1016/j.watres.2023.120714

Zeng, X., Sun, X., Meng, Y., et al. 2021. Photodegradation of Sulfamethoxypyridazine in UV/Co(II)/peroxymonosulfate System: Kinetics, influencing factors, degradation pathways, and toxicity assessment. Water, Air, Soil Pollut. 232(10), 410. https://doi.org/10.1007/s11270-021-05351-5

Jung, J., Kim, Y., Kim, J., et al. 2008. Environmental levels of ultraviolet light potentiate the toxicity of sulfonamide antibiotics in *Daphnia magna*. Ecotoxicology (London, England) 17(1), 37-45. https://doi.org/10.1007/s10646-007-0174-9

Xu, J., Hao, Z., Guo, C., et al. 2014. Photodegradation of sulfapyridine under simulated sunlight irradiation: Kinetics, mechanism and toxicity evolvement. Chemosphere 99, 186-191. https://doi.org/10.1016/j.chemosphere.2013.10.069

Trovó, A.G., Nogueira, R.F.P., Agüera, A., et al. 2009. Photodegradation of sulfamethoxazole in various aqueous media: Persistence, toxicity and photoproducts assessment. Chemosphere 77(10), 1292-1298. https://doi.org/10.1016/j.chemosphere.2009.09.065

Voigt, M., Bartels, I., Nickisch-Hartfiel, A., et al. 2017. Photo-induced degradation of sulfonamides, kinetic and structural characterization of transformation products, and assessment of environmental toxicity. Toxicol. Environ. Chem. 99, 01-29. https://doi.org/10.1080/02772248.2017.1373777

Zessel, K., Mohring, S., Hamscher, G., et al. 2014. Biocompatibility and antibacterial activity of photolytic products of sulfonamides. Chemosphere 100, 167-174. https://doi.org/10.1016/j.chemosphere.2013.11.038

Mac Loughlin, T.M., Bahl, M.F., Flores, F.M., et al. 2024. Assessment of sulfonamide contamination in aquatic environments: A first report for Argentina and environmental risk assessment. Sci. Total Environ. 934, 173139. https://doi.org/10.1016/j.scitotenv.2024.173139

Ge, L., Cao, S., Halsall, C., et al. 2023. Photodegradation of hydroxyfluorenes in ice and water: A comparison of kinetics, effects of water constituents, and phototransformation by-products. J.Environ.Sci. 124, 139-145. https://doi.org/10.1016/j.jes.2021.11.002

Luo, X., Wei, X., Chen, J., et al. 2019. Rate constants of hydroxyl radicals reaction with different dissociation species of fluoroquinolones and sulfonamides: Combined experimental and QSAR studies. Water Res. 166, 115083. https://doi.org/10.1016/j.watres.2019.115083

Cui, J., Chen, Y., Cheng, F., et al. 2025. Hydrophilicity-dependent photodegradation of antibiotics in ice: Freeze-concentration effects and dissolved organic matter interactions drive divergent kinetics, pathways and toxicity. Water Res. 286, 124277. https://doi.org/10.1016/j.watres.2025.124277

Ge, L., Na, G., Zhang, S., et al. 2015. New insights into the aquatic photochemistry of fluoroquinolone antibiotics: Direct photodegradation, hydroxyl-radical oxidation, and antibacterial activity changes. Sci. Total Environ. 527-528, 12-17. https://doi.org/10.1016/j.scitotenv.2015.04.099

543 Tao, R., Ying, G.-G., Su, H.-C., et al. 2010. Detection of antibiotic resistance and tetracycline
544 resistance genes in *Enterobacteriaceae* isolated from the Pearl rivers in South China.
545 Environ. Pollut. 158(6), 2101-2109. https://doi.org/10.1016/j.envpol.2010.03.004
546 Klančnik, A., Piskernik, S., Jeršek, B., et al. 2010. Evaluation of diffusion and dilution methods
547 to determine the antibacterial activity of plant extracts. J. Microbiol. Methods 81(2), 121-
548 126. https://doi.org/10.1016/j.mimet.2010.02.004
549 Boreen, A.L., Arnold, W.A. and McNeill, K. 2005. Triplet-sensitized photodegradation of sulfa
550 drugs containing six-membered heterocyclic groups: Identification of an SO_2 extrusion
551 photoproduct. Environ. Sci. Technol. 39(10), 3630-3638.
552 https://doi.org/10.1021/es048331p
553 Boreen, A.L., Arnold, W.A. and McNeill, K. 2004. Photochemical fate of sulfa drugs in the
554 aquatic environment: Sulfa drugs containing five-membered heterocyclic groups. Environ.
555 Sci. Technol. 38(14), 3933-3940. https://doi.org/10.1021/Es0353053
556 Zhou, L., Yang, X., Ji, Y., et al. 2019. Sulfate radical-based oxidation of the antibiotics
557 sulfamethoxazole, sulfisoxazole, sulfathiazole, and sulfamethizole: The role of five-
558 membered heterocyclic rings. Sci. Total Environ. 692, 201-208.
559 https://doi.org/10.1016/j.scitotenv.2019.07.259
560 Ge, L., Wang, S., Cui, N., et al. 2025a. Insight into the environmental photochemistry of nitrated
561 polycyclic aromatic hydrocarbons in water and in ice: Kinetics, pathways and photo-
562 modified toxicity. Environ. Res. 279, 121749.
563 https://doi.org/10.1016/j.envres.2025.121749
564 Kolasinski, K.W. 2025. Radical surface chemistry: Augmentation of reactivity by radicals at
565 aqueous interfaces. Surf. Sci. Rep. 80(4), 100668.
566 https://doi.org/10.1016/j.surfrep.2025.100668
567 Ge, L., Zheng, J., Halsall, C., et al. 2024. Aquatic photo-transformation and enhanced
568 photoinduced toxicity of ionizable tetracycline antibiotics. Front. Environ. Sci. Eng.
569 18(11). https://doi.org/10.1007/s11783-024-1899-x
570 Shah, S. and Hao, C. 2017. Quantum chemical investigation on photodegradation mechanisms
571 of sulfamethoxypyridazine with dissolved inorganic matter and hydroxyl radical. J.
572 Environ. Sci. 57, 85-92. https://doi.org/10.1016/j.jes.2016.09.023
573 Bilea, F., Bradu, C., Cicirma, M., et al. 2024. Plasma treatment of sulfamethoxazole
574 contaminated water: Intermediate products, toxicity assessment and potential agricultural
575 reuse. Sci. Total Environ. 909, 168524. https://doi.org/10.1016/j.scitotenv.2023.168524

Ji, Y., Shi, Y., Wang, L., et al. 2017. Sulfate radical-based oxidation of antibiotics sulfamethazine, sulfapyridine, sulfadiazine, sulfadimethoxine, and sulfachloropyridazine: Formation of SO_2 extrusion products and effects of natural organic matter. Sci. Total Environ. 593-594, 704-712. https://doi.org/10.1016/j.scitotenv.2017.03.192

Hernández-Tenorio, R. 2024. Degradation pathways of sulfamethoxazole under phototransformation processes: A data base of the major transformation products for their environmental monitoring. Environ. Res. 262(Pt 1), 119863. https://doi.org/10.1016/j.envres.2024.119863

Loureiro Dos Louros, V., Silva, C.P., Nadais, H., et al. 2020. Photodegradation of sulfadiazine in different aquatic environments - Evaluation of influencing factors. Environ. Res. 188, 109730. https://doi.org/10.1016/j.envres.2020.109730

Qin, X., Liu, X., He, Y., et al. 2024. Kinetic modeling of sulfonamide degradation by UV/H_2O_2: Deduction of $R_{OH,UV}$ modeling and application. Chemosphere 369, 143836. https://doi.org/10.1016/j.chemosphere.2024.143836

Niu, X.Z., Glady-Croué, J. and Croue, J.P. 2017. Photodegradation of sulfathiazole under simulated sunlight: Kinetics, photo-induced structural rearrangement, and antimicrobial activities of photoproducts. Water Res. 124, 576-583. https://doi.org/10.1016/j.watres.2017.08.019

Baek, S., Joo, S.H., Su, C., et al. 2019. Antibacterial effects of graphene- and carbon-nanotube-based nanohybrids on Escherichia coli: Implications for treating multidrug-resistant bacteria. J. Environ. Manag. 247, 214-223. https://doi.org/10.1016/j.jenvman.2019.06.077

Huang, S., Zhang, X., Qin, H., et al. 2025. The impact of light parameters and tetracycline concentration on antimicrobial photodynamic inactivation against drug resistant *Escherichia coli*. J. Biophotonics 18(9), e70049. https://doi.org/10.1002/jbio.70049

Guo, Z., Zhang, T., Yang, H., et al. 2025b. Unraveling tetracycline and its degradation product: Induction mechanisms of antibiotic resistance in *Escherichia coli*. Sci. Total Environ. 970, 178959. https://doi.org/10.1016/j.scitotenv.2025.178959

Ge, P., Liu, N., Wang, Y., et al. 2025b. Isomer-specific ecotoxicity and occurrence of ibuprofen: Underestimated risks in aquatic ecosystems. J. Hazard. Mater. 496, 139430. https://doi.org/10.1016/j.jhazmat.2025.139430

Ge, L., Hou, Z., Niu, J., et al. 2025c. New insights into the environmental photochemistry of hydroxynaphthalene congeners in water and in ice: A distinct comparative study. J. Hazard. Mater. 493, 138310. https://doi.org/10.1016/j.jhazmat.2025.138310

609 Jablonski, E. and DeLuca, M. 1978. Studies of the control of luminescence in Beneckea harveyi:
610 properties of the NADH and NADPH: FMN oxidoreductases. Biochemistry 17(4), 672-
611 678. https://doi.org/10.1021/bi00597a018
612 Park, J.-A., Pineda, M., Peyot, M.-L., et al. 2023. Degradation of oxytetracycline and
613 doxycycline by ozonation: Degradation pathways and toxicity assessment. Sci. Total
614 Environ. 856, 159076. https://doi.org/10.1016/j.scitotenv.2022.159076
615 Zheng, J., Niu, J., Halsall, C., et al. 2025. New insights into transformation mechanisms for
616 sulfate and chlorine radical-mediated degradation of sulfonamide and fluoroquinolone
617 antibiotics. Chin. Chem. Lett. 36(5), 110202. https://doi.org/10.1016/j.cclet.2024.110202
618 Felis, E., Sochacki, A., Bajkacz, S., et al. 2024. Removal of selected sulfonamides and
619 sulfonamide resistance genes from wastewater in full-scale constructed wetlands. Sci.
620 Total Environ. 912, 169195. https://doi.org/10.1016/j.scitotenv.2023.169195
621 Duan, W., Cui, H., Jia, X., et al. 2022. Occurrence and ecotoxicity of sulfonamides in the aquatic
622 environment: A review. Sci. Total Environ. 820, 153178.
623 https://doi.org/10.1016/j.scitotenv.2022.153178
624 Li, J., Peng, X., Zeng, P., et al. 2025b. Removal of sulfonamides by persulfate-based advanced
625 oxidation: A mini review. Chemosphere 370, 143874.
626 https://doi.org/10.1016/j.chemosphere.2024.143874